Atmósfera (1996), **9**, *pp. 223-240*

A note on longer term oscillations in the atmosphere

AKSEL WIIN-NIELSEN

Department of Geophysics University of Copenhagen Juliane Maries Vej 30 2100 Copenhagen Ø, Denmark

RESUMEN

Se usa un modelo simple, no-lineal, de orden bajo, con forzamiento y disipación para demostrar que las oscilaciones intermensuales pueden ser ocasionadas por la interacción no-lineal. La longitud del periodo depende de la intensidad del forzamiento.

El modelo empleado en las integraciones tiene tres componentes.

Otro modelo de orden bajo, basado en la ecuación de vorticidad barotrópica con forzamiento newtoniano se utiliza para demostrar que unas oscilaciones semejantes aparecen también en este modelo.

Se propone que los modelos pueden describir el mecanismo básico de las variaciones atmosféricas intermensuales observadas, aunque los modelos son demasiado sencillos para tomar en cuenta los detalles en las distribuciones espaciales de las variaciones.

ABSTRACT

A simple low-order nonlinear model with forcing and dissipation is used to demonstrate that inter-monthly oscillations may be caused by the nonlinear interaction. The length of the period depends on the intensity of the forcing. The model used for the integrations has three components.

Another low-order model based on the barotropic vorticity equation with Newtonian forcing is used to show that similar oscillations appear also in this model.

It is proposed that the models may describe the basic mechanism for the observed atmospheric intermonthly variations although the models are too simple to account for details in the spatial distributions of the variations.

1. Introduction

Since Madden and Julian (1971) detected a 40-50 day oscillation in the zonal wind in the tropical Pacific it has been possible to describe other spells of oscillations in the extratropical latitudes. A large observational study conducted by Plaut and Vautard (1994) has described several low frequency oscillations. Using 32 years of 700 hPa maps for the Northern Hemisphere it was possible to describe three major oscillations. The 70 day oscillation consists of fluctuations in both position and amplitude of the Atlantic jet. The 40-45 day oscillation is found in the Pacific sector. In its high amplitude phase it is similar to what has been called the Pacific/North American (PNA) structure, while the 30-35 day oscillation is found in the Atlantic region and is described as a retrograding dipole pattern. It is also speculated that the 30-35 day oscillation is a sub-harmonic of the 70 day oscillation. For all the oscillations it should be mentioned that they are excited from time to time pointing to the importance of the forcing.

The study by Plaut and Vautard (*loc.cit.*) relates the occurrence of blocking to the life cycle of the 30-35 day oscillation and thus to the importance of the forcing permitting radical changes of the flow pattern.

The low frequency oscillations have been classified in terms of the associated large-scale anomalies by Wallace and Gutzler (1981). These studies result in a description of teleconnection patterns that contain a large part of the variability. Empirical orthogonal functions (Barnett and Preisendorfer, 1987, Mo and Ghil, 1987 and Preisendorfer, 1988) are used to describe the teleconnection patterns. They have also been described using cluster analysis (Legras *et al.*, 1987, Mo and Ghil, 1988, Molteni *et al.*, 1990).

Quasi-stationary weather pattern have been identified by the use of low-order models by Reinhold and Pierrehumbert (1982) and Vautard and Legras (1988). It may thus be said that the low frequency extratropical atmosphere has a preference for a low number of quasi-stationary states, and that a change in weather regimes normally is a change from one preferred state to another.

We have thus a good knowledge of the spatial distribution of the low frequency oscillations, and as described above the observational studies have also resulted in the determination of the time scales involved in them.

On the theoretical side we prefer to describe matters using the dynamical system theory for forced and dissipative systems where it is assumed that the number of possible states occurring after a long integration is small. The set of states may be as simple as a point in phase space, a stable periodic orbit, normally called a limit cycle, or an aperiodic behavior called a strange attractor. The latter is connected with chaos and is equivalent to limited predictability (Lorenz, 1963).

Quasi-stationary behavior is observed in the middle latitudes, where certain regimes may persist over a long time such as for example the blocking situations. The first theories of blocking were given by Charney and DeVore (1979) and Wiin-Nielsen (1979) using different low-order models where the mountain forcing was emphasized in the former study of a model on the beta plane, while the forcing by heating was used in the latter study using a low order model on the spherical Earth. However, in both cases the blocking pattern was established through interactions between the zonal flow and the eddies. A later study by Wiin Christensen and Wiin-Nielsen (1996) showed that the blocking pattern could just as well be established by interaction between the three longest planetary waves without the participation of the zonal flow. Weather regimes have also been found by Legras and Ghil (1985) and Itoh (19985) as stationary solution of simplified general circulation models.

Low frequency oscillations are classified in the three categories:

1. intramonthly oscillations with periods of less than a month (blocking belongs to this category although they may occasionally persist for longer times),

2. intermonthly oscillations with periods from a month to a year, also occasionally called interseasonal oscillations,
3. interannual variations with periods of more than a year,
4. interdecadal oscillations.

In the present study we shall be particularly interested in the intermonthly oscillations where the time scales have been established by observational studies. As pointed out above these oscillations are influenced by the forcing. It is thus of considerable interest to investigate the mechanism that may be responsible for the observed time scales of the intermonthly oscillations. This time scale is certainly much larger than the time scale of the baroclinic instability of the transient waves including the largest time scale connected with the weak instability of the planetary waves of the order of 5-10 days. The dissipation time scale is also shorter than the time scale for the oscillations in question. Since a time scale of the desired order of magnitude does not seem to appear from any solution of the linear equations it would appear that we have to deal with nonlinear models.

The present study will use an extremely simple model for nonlinear interactions first developed by Wiin-Nielsen (1975) to illustrate the existence of multiple steady states and the dependence of the stability of these states on the magnitude of the external forcing. The original study is in certain regards similar to, but independent of the early work by Obukhov (1974) who also worked with simple nonlinear models to explain certain laboratory experiments.

In the present context we shall use a minimum truncation that will permit the existence of limit cycles. These models have also been analysed by Källén and Wiin-Nielsen (1980). Among the many solutions of the model equations, each dependent on the magnitude of the forcing on the various components, we shall be particularly interested in those cases where all steady states are unstable preventing the model from approaching a point in the phase space in the asymptotic limit. Since the model can be shown to be stable in the sense that it cannot go to infininity in phase space, and since no stable steady states exist, we can expect the model to have either a stable limit cycle or behave as a strange attractor. If that is the case we shall also be able to determine the typical time scale for the periodic or aperiodic behavior and thus be able to see whether or not the time scales are of the same order of magnitude as the various time scales observed in the low frequency oscillations in the atmosphere. The forcing will in any model influence the time scale. We can therefore not expect that only the observed periods will be present in the model.

2. The model

The model is derived from a one-dimensional version of the equations of motion. We permit one space coordinate (x) and the time (t) dependence. We add forcing in a Newtonian way including the dissipation. The Newtonian term may be considered as a simple modeling of the momentum forcing, but it is also an easy way to write a constant forcing and a dissipation that is proportional to the velocity, u. The model equation may be written in the form:

$$\frac{\partial u}{\partial t} + u\frac{\partial u}{\partial x} = \gamma(u_E - U) \tag{2.1}$$

where u is a velocity component and γ is a coefficient of dimension t^{-1}. Considering the modeling of the boundary layer friction in the atmosphere we should use a value $\gamma \approx 1 \times 10^{-6} s^{-1}$ corresponding to a time scale of about 11.6 days. The numerical value of the coefficient can be determined by assuming a boundary layer dissipation only and assuming that the surface

stress is proportional to the surface density and to a standard value of the surface wind. This formulation gives the above value of γ, if one uses an equivalent barotropic model as the basis for the determination. It is realized that the determination is uncertain depending on the choices of the various parameters. By using this formulation we have not provided a time scale of the order of magnitude of any of the intermonthly oscillations.

It will be convenient for our purposes to convert (2.1) to the spectral domain. For this purpose and to keep the calculations simple we use a representation for u as follows:

$$u(x,t) = \sum_{n=1}^{N} u(n,t)\sin(nkx) \tag{2.2}$$

where k is the basic wave number. Inserting (2.2) in (2.1) we obtain an equation in wave number space. In deriving the following equation we have calculated the interaction coefficients directly. The resulting equation is:

$$\frac{du(n)}{dt} = 1/2nk \sum_{q=1}^{N-n} u(q)u(n+q) - 1/2k \sum_{q=1}^{n-1} qu(q)u(n-q) + \gamma(u_E(n) - u(n)) \tag{2.3}$$

Eq. (2.3) can be integrated as it stands by selecting the maximum wave number N and numerical values for k and γ. However, it is more convenient for the later integrations to non-dimensionalize the equation. For this purpose we define a length scale $L = 1/k$, a time scale T and a velocity scale U.

Inserting in (2.3) we find that

$$T = \frac{1}{\gamma}; U = 2L\gamma \tag{2.4}$$

Denoting $w(n) = u(n)/U$ and $\tau = t/T$ we find that the basic equation becomes:

$$\frac{dw(n)}{d\tau} = n \sum_{q=1}^{N-n} w(q)w(n+q) - \sum_{q=1}^{n-1} qw(q)w(n-q) + w_E(n) - w(n) \tag{2.5}$$

We shall consider a low-order system with $N = 3$. Denoting $w(1) = x$, $w(2) = y$ and $w(3) = z$ we find the following three equations:

$$\frac{dx}{d\tau} = xy + yz + x_E$$

$$\frac{dy}{d\tau} = 2xz - x^2 + y_E - y$$

$$\frac{dz}{d\tau} = -3xy + z_E - z \tag{2.6}$$

This system in a slightly different formulation has been considered by Källén and Wiin-Nielsen

(1980). For the equations (2.6) we are seeking the steady states. From the third of the equations we find that

$$z = z_e - 3xy \tag{2.7}$$

Inserting from (2.7) in the second equation of (2.6) we may solve for y with the result:

$$y = \frac{2z_E x - x^2 + y_E}{1 + 6x^2} \tag{2.8}$$

Eliminating y and z from the first equation in (2.6) we obtain finally a single equation in the variable x. It can be solved numerically in a number of ways, and it is:

$$(2z_e x - x^2 + y_E)[(1 + 6x^2)(x + z_E - 3x(2z_E x - x^2 + y_E)]+$$

$$+(1 + 6x^2)^2(x_E - x) = 0 \tag{2.9}$$

Once the steady states are known one can determine the stability of each of them. Linearizing the three time-dependent equations in (2.6) around a steady state it is a straightforward matter to determine the eigenvalues by numerical methods. As mentioned in the introduction we shall in general be interested in cases in which all the steady states are unstable. However, limit cycles may actually also be present in other cases. Assume for example that we have two unstable and one stable steady state. As long as the initial state for the integration can be selected in such a way that it is outside the attractor basin of the stable steady state one will be able to determine the behavior of the system as determined by the two unstable steady states.

3. Results of the three component model

We shall start by considering the most simple case. It is assumed that $x_E = z_E = 0$, but $y_E > 0$. The solution for the steady state is especially simple in this case, and it is found that

$$\overline{x} = \overline{z} = 0; \overline{y} = y_E \tag{3.1}$$

Considering next the stability of the steady state it is found that it is unstable, if $y_E > 2$. When the inequality is satisfied we have thus a possibility for a limit cycle. The full equations were integrated for $y_E = 3$. The results are shown in Figures 1a, 1b, 1c and 1d. Figure 1a shows a very simple time dependence of one of the dependent variables on time. Converting the nondimensional coordinate to real time we find a period of about 22.5 days. The experiment shows then that relatively large time scales for the limit cycle are possible. Figures 1b, 1c and 1d show the projection of the three-dimensional limit cycle on the xy, the xz and the yz planes indicating that the limit curve is relatively simple. This behavior is, however, the exception rather than the rule.

Numerical experiments show that the time scales remain the same (22.5 days) for values of $y_E < 4.890$. For values of y_E satisfying the inequality $4.890 \leq y_E \leq 5.165$ we observed larger time scales.

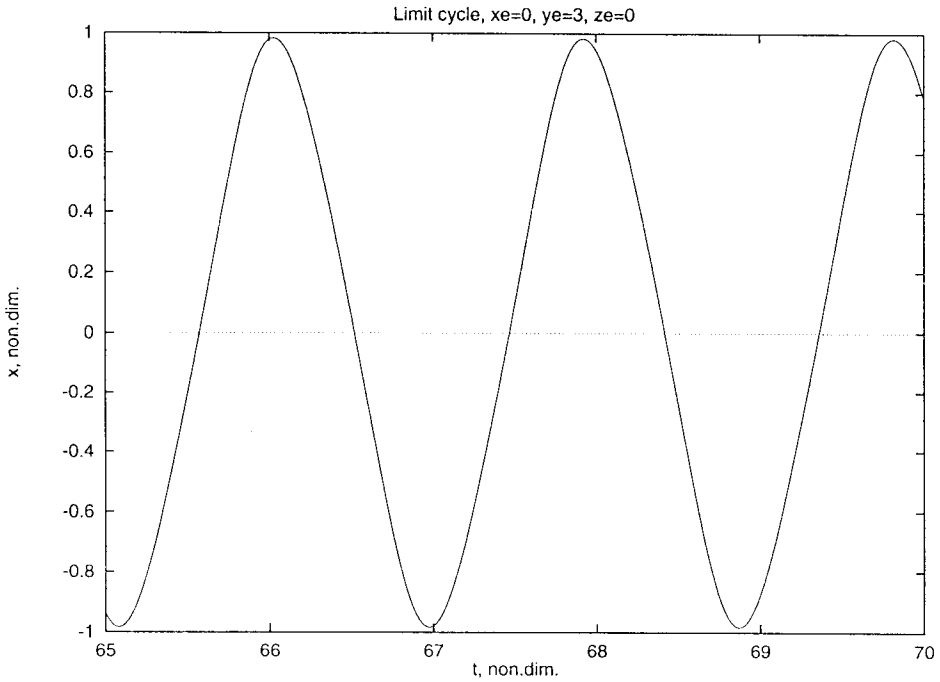

Fig. 1a. The amplitude of the x-component as a function of time with $x_E = 0$, $y_E = 3$ and $z_E = 0$. The period is about 23 days.

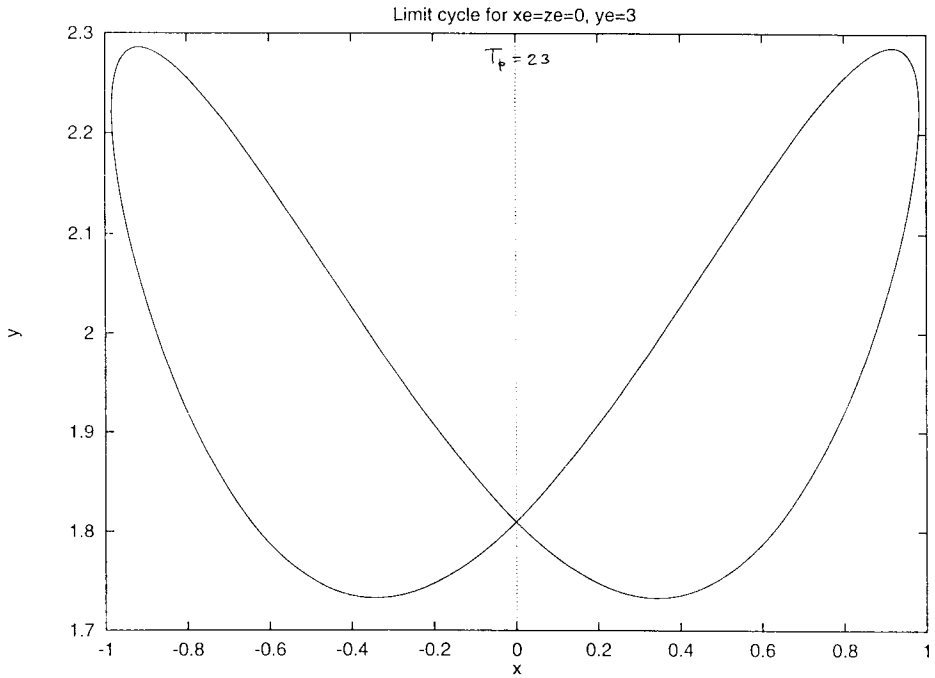

Fig. 1b. The projection of the limit cycle on the xy-plane. Parameters as in Fig. 1a.

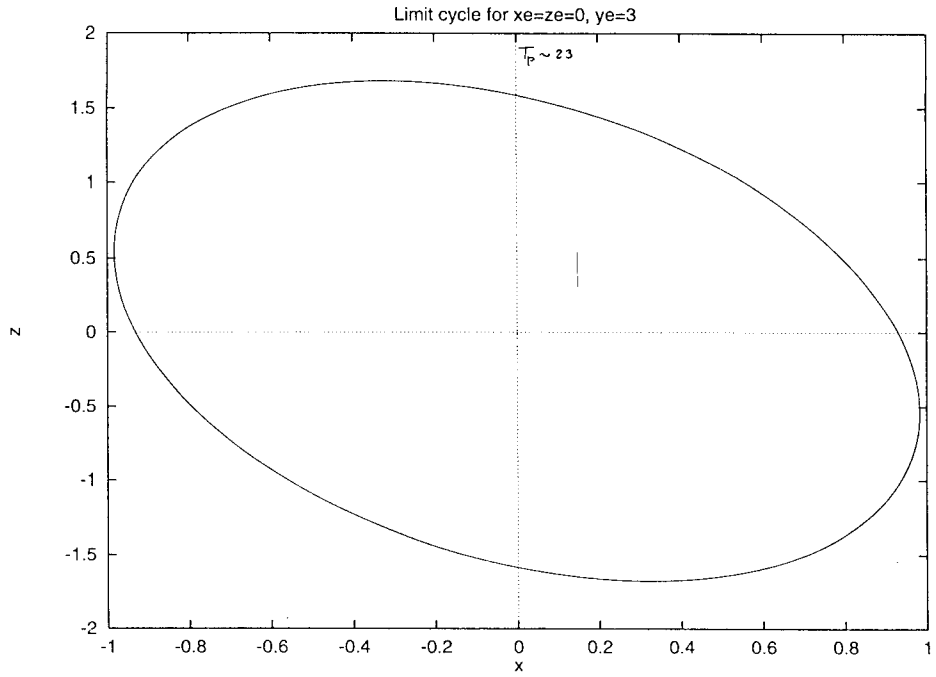

Fig. 1c. The projection of the limit cycle on the xz-plane.

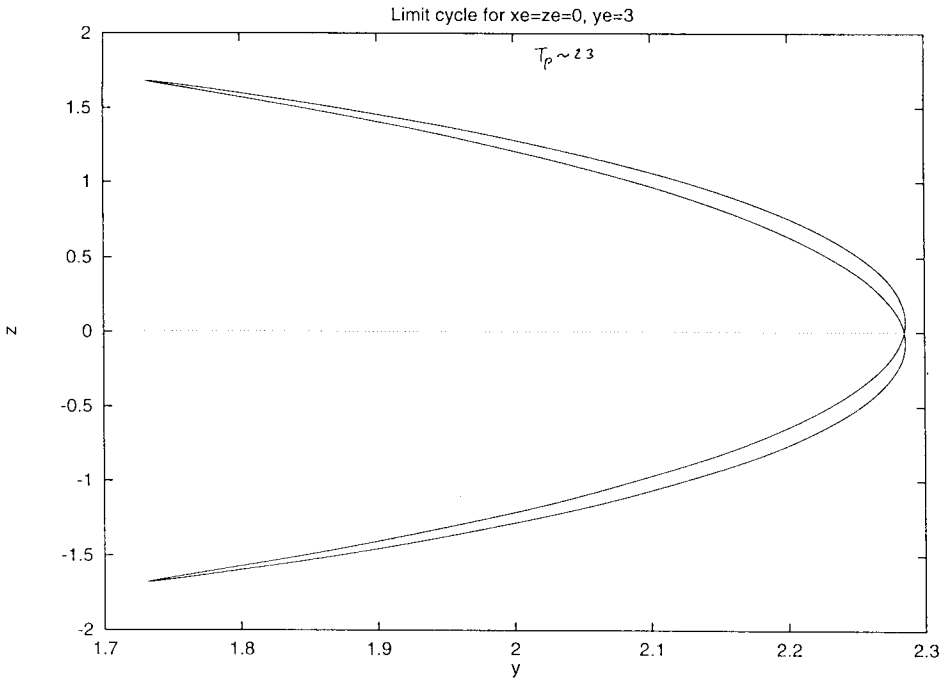

Fig. 1d. The projection of the limit cycle on the yz-plane.

The next case has $x_E = z_E = 0$ and $y_E = 5$. From Figure 2a it is seen that the non-dimensional period is about 3.9 corresponding to close to 45 days. Fig. 2b, showing the projection of the limit curve on the xy-plane, indicates that the stable limit cycle is becoming more complicated.

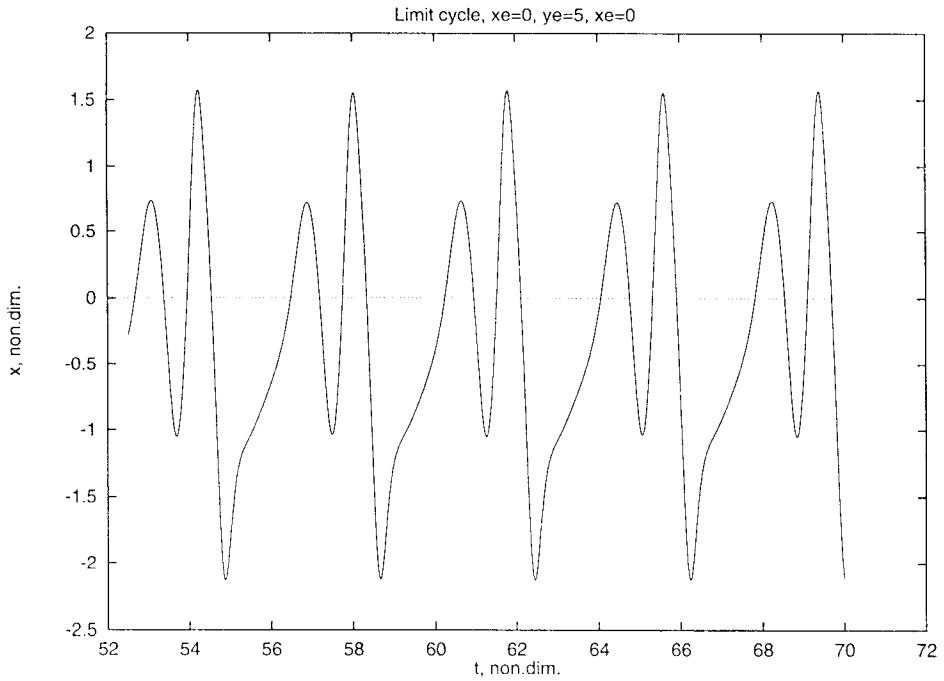

Fig. 2a. The amplitude of the x-component as a function of time with $x_E = 0$, $y_E = 5$ and $z_E = 0$. The amplitude is about 45 days.

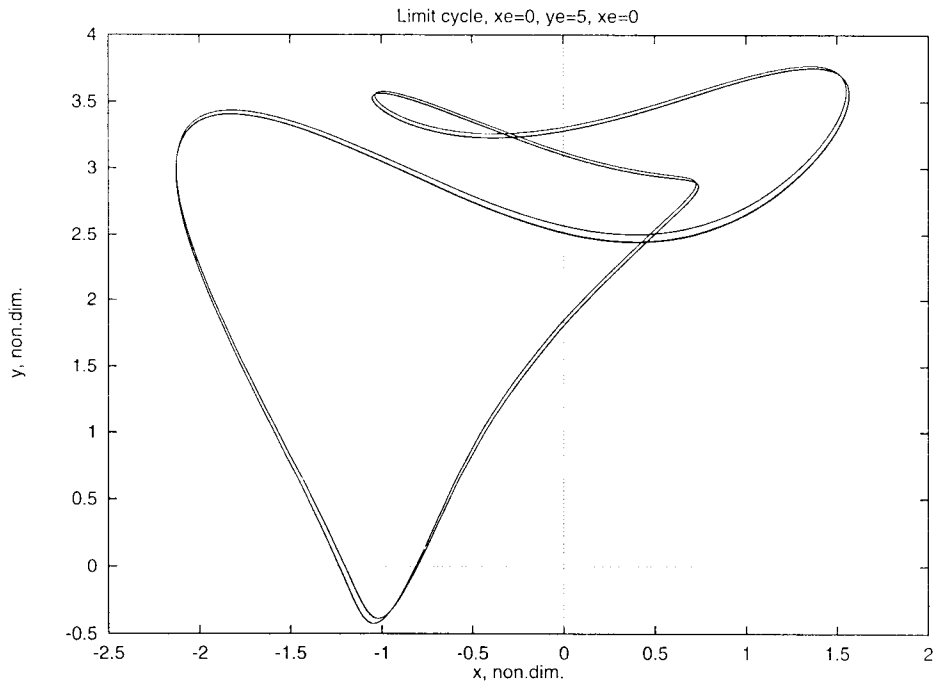

Fig. 2b. The projection of the limit cycle on the xy-plane. The figure indicates two slightly different half periods. Parameters as in Fig. 2a.

The forcing is determined by the three values for x_E, y_E and z_E. Since the limit cycle can be determined by numerical integration only, it is possible, but cumbersome to investigate the period of the limit cycle over a large volume of the forcing parameters, but this will not be done in the present investigation. However, when $x_E = 0$ and $z_E = 0$ we find by numerical experimentation that when y_E is larger 5.165 the period of the oscillation returns to 22.5 days. The short period disappears when y_E is about 6.5, when the larger time scales appear again. As an example we show x as function of time for $x_E = 0$, $y_E = 7.5$ and $z_E = 0$ in Figure 3. In the figure one observes a large and a small time scale. They correspond to 30 and 67 days.

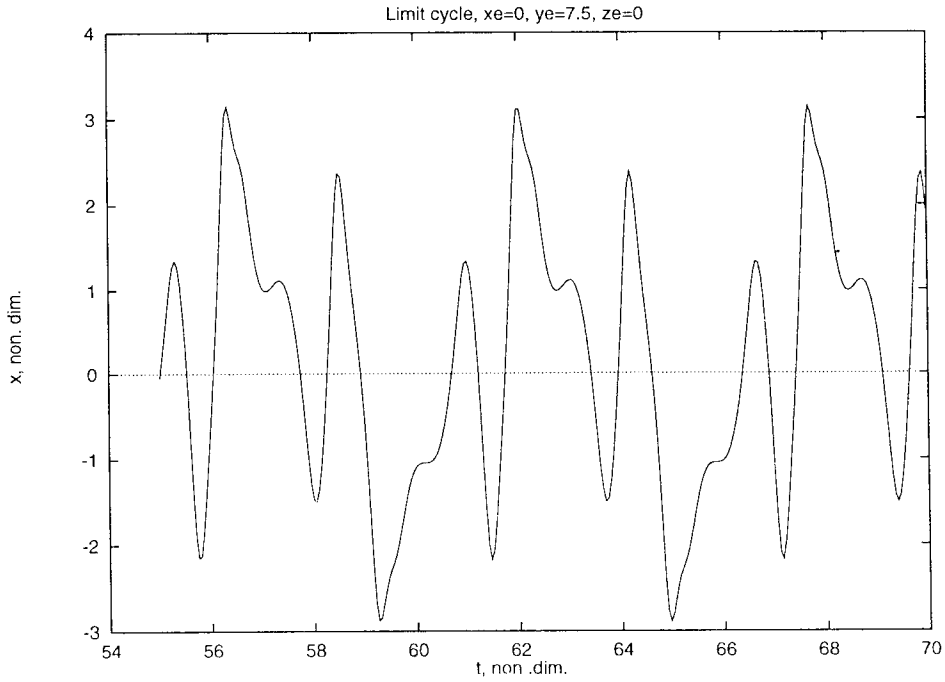

Fig. 3. The amplitude of the x-component as a function of time with $x_E = 1$, $y_E = 5$ and $z_E = 1$. The period is about 70 days.

By selecting suitable examples we can, however, show that the behavior of the model is strongly dependent on the values of the forcing parameters. Figures 4a and 4b are obtained for $x_E = 1$, $y_E = 5$ and $z_E = 1$. As seen from Figure 4a we get a much longer period for the limit cycle. Converting to dimensional time we find a period of close to 70 days. Figure 4b shows the projection of the limit curve on the xy-plane.

So far we have shown examples having periods of 22.5, 30, 45 and 70 days. Similar results may be obtained for large values of the forcing. Figures 5a and 5b show the results of an integration with $x_E = 1.25$, $y_E = 10.0$, and $z_E = 1.25$. As one will observe in Figure 5a, the real period is quite long (about 68 days), but it is divided on two time scales of 32 and 36 days. Figure 5b shows the projection on the xy-plane.

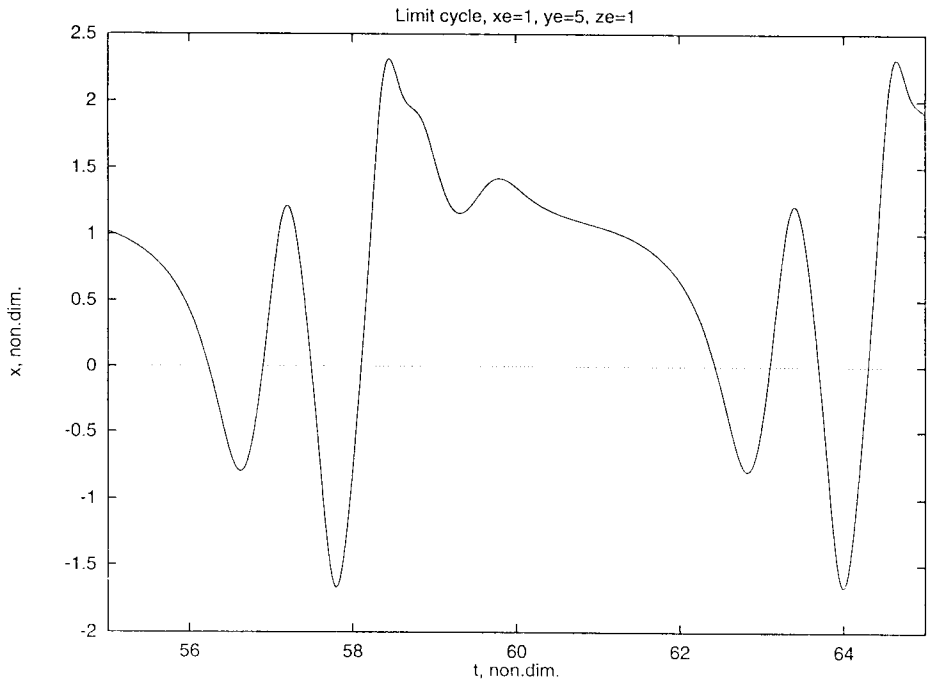

Fig. 4a. The amplitude of the x-component as a function of time with $x_E = 1.25$, $y_E = 10.0$ and $z_E = 1.25$. Two timescales are present. They corresponds to 32 and 36 days giving a period of 68 days.

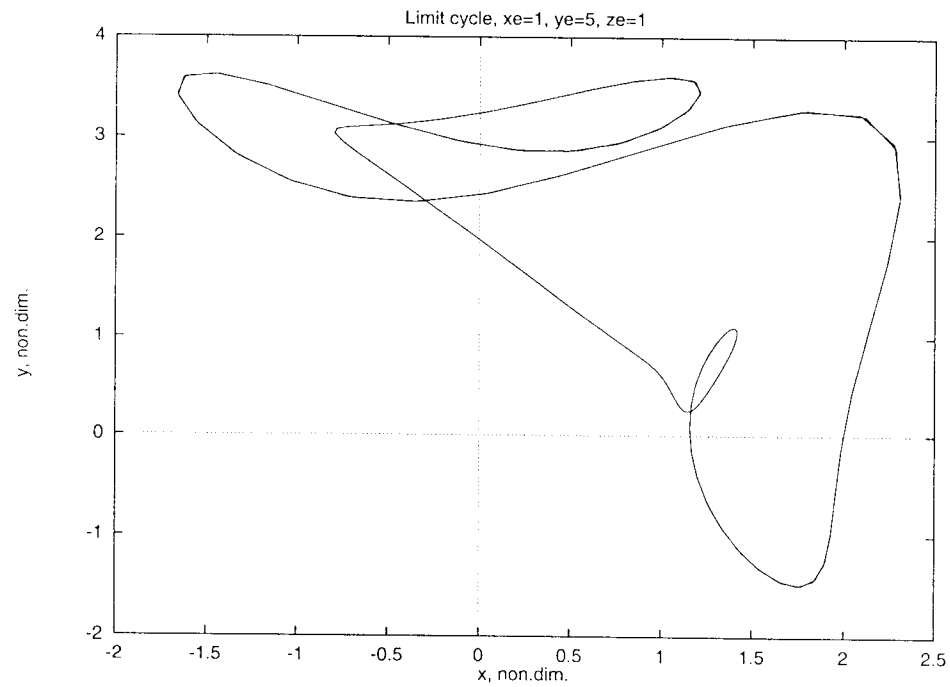

Fig. 4b. The projection of the limit cycle on the xy-plane. The two time scales are seen as two loops in the periodic trajectory.

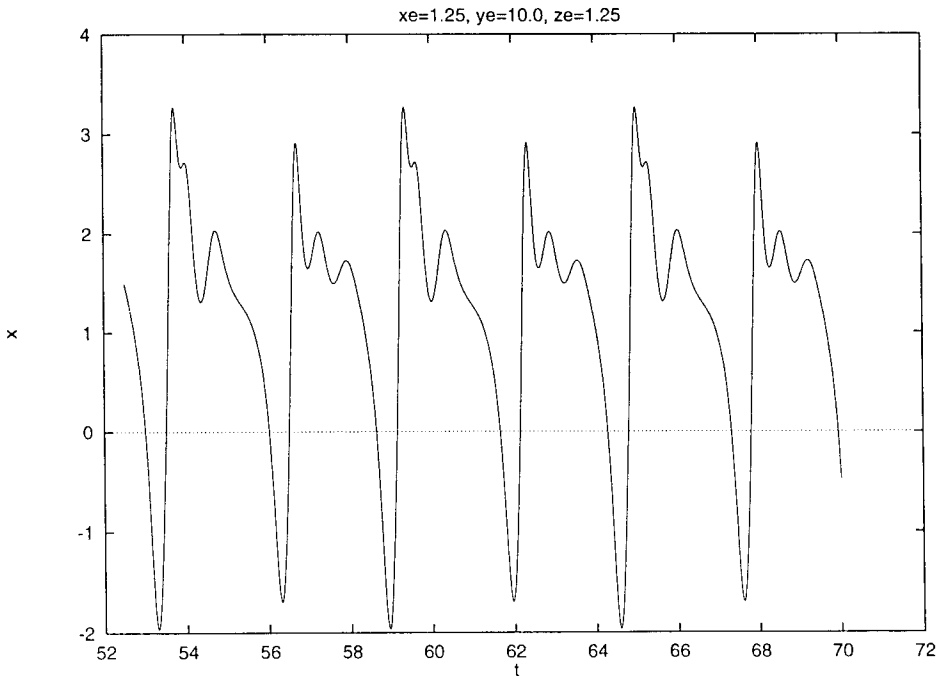

Fig. 5a. The amplitude of the x-component as a function of time with $x_E = 1.5$, $y_E = 10.0$ and $z_E = 1.5$. The period is about 46 days.

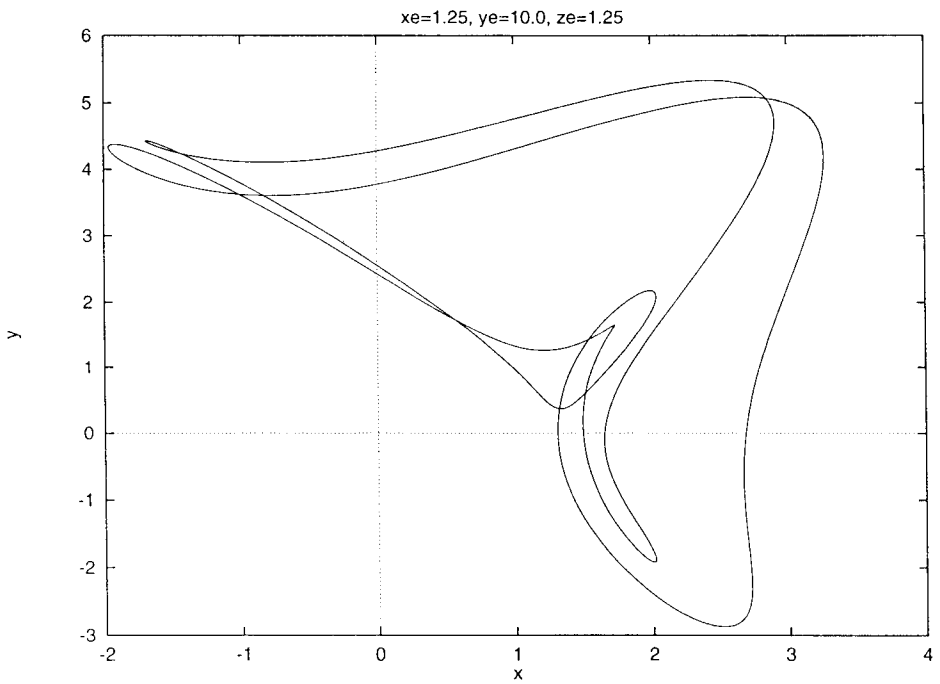

Fig. 5b: Projection of the limit cycle on the xy-plane.

Using the same order of magnitude for the forcing we may also reproduce the other time scales found from the observational studies. Figures 6a and 6b are calculated for $x_E = 1.5$, $y_E = 10.0$ and $z_E = 1.5$. The single period in Figure 6a converts to about 46 days, while Figure 6b as before is the projection of the limit curve on the xy-plane. Figure 7a computed for $x_E = 1.65$, $y_E = 10.0$ and $z_E = 1.65$ has a single period corresponding to about 69 days. It is thus seen that relatively minor changes in the forcing will have large impacts on the period of the limit cycle.

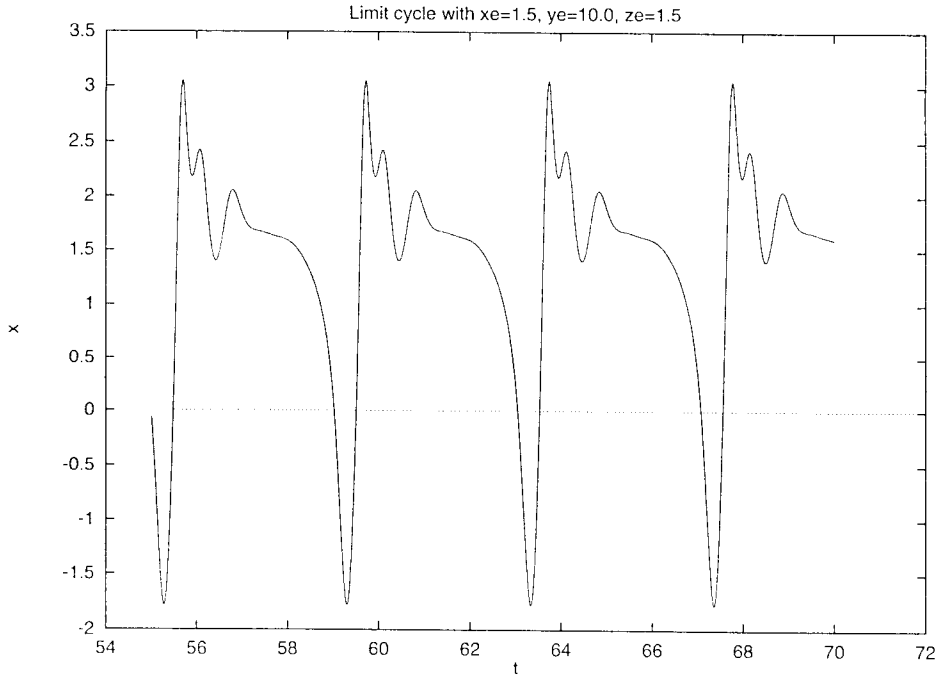

Fig. 6a. The amplitude of the x-component as a function of time with $x_E = 1.65$, $y_E = 10.0$ and $z_E = 1.65$. The period is about 69 days.

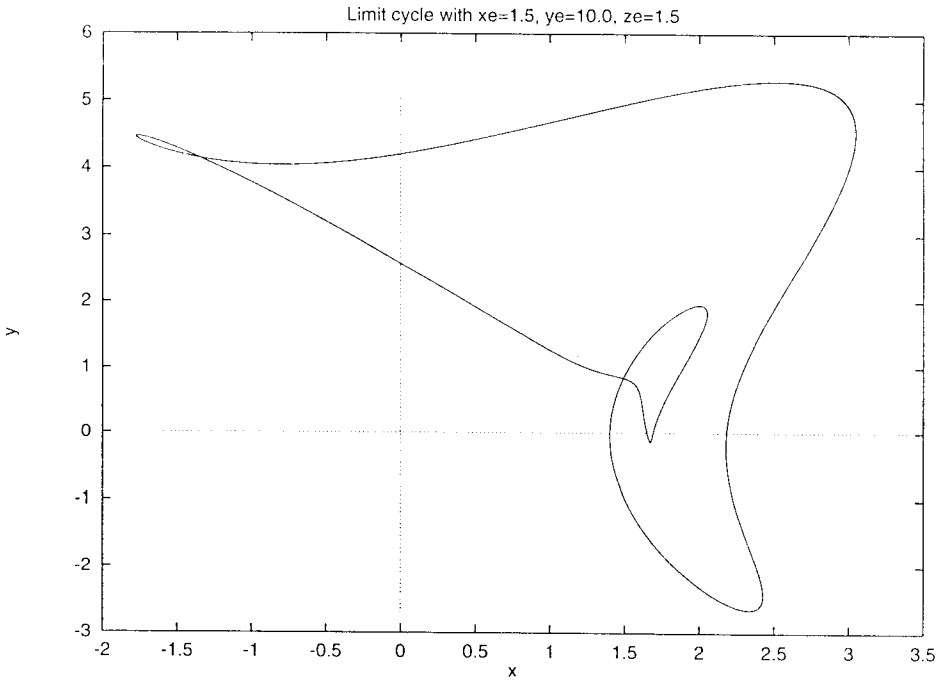

Fig. 6b. The projection of the limit cycle on the xz-plane.

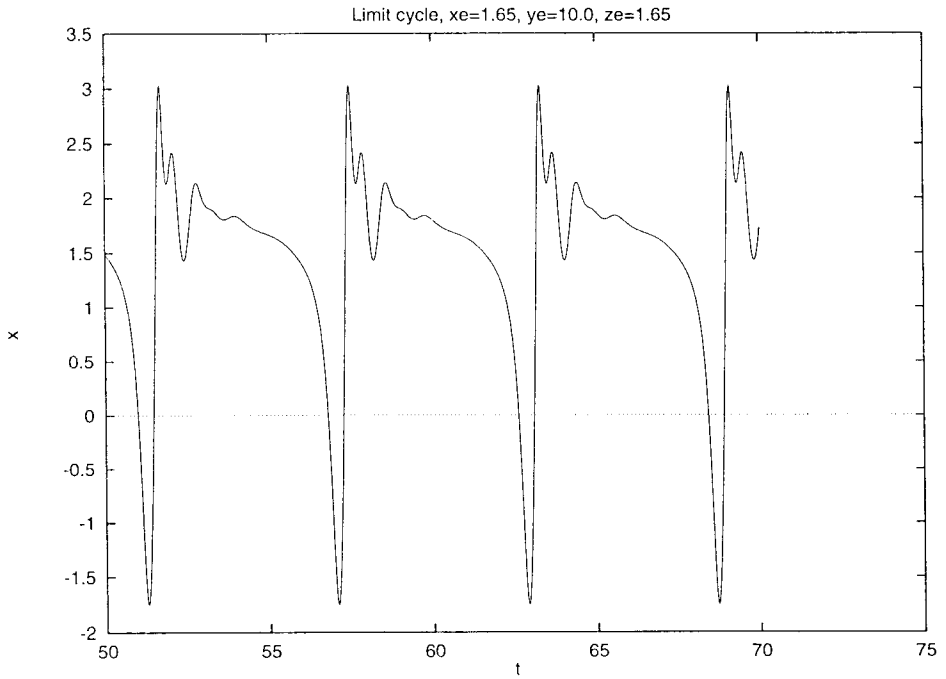

Fig. 7a. Another case with two time scales of 35 and 69 days for $x_E = 1$, $y_E = 12$ and $z_E = 1$. The amplitude of the x-component as a function of time.

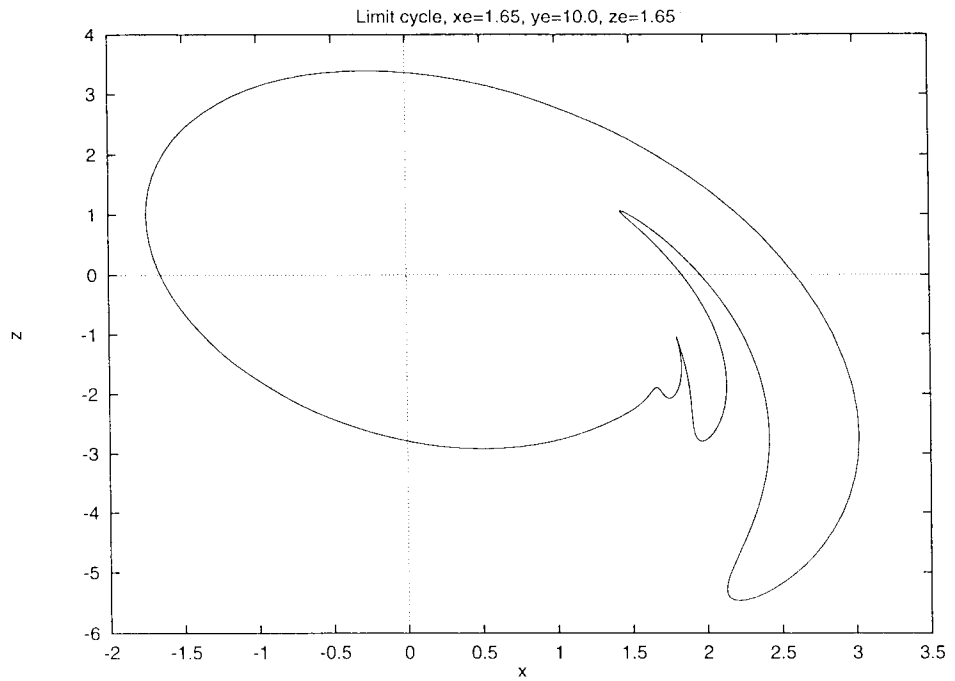

Fig. 7b. The projection of the limit cycle on the xz-plane. The two time scales are seen.

As a minor variation we show this time in Figure 7b the projection of the limit cycle on the xz-plane. To illustrate the two time scales that may be present in individual cases we present a case with $x_E = 1.0$, $y_E = 12.0$ and $z_E = 1.0$. Figure 8a shows clearly the two timescales in the integration after a long time. They correspond to 35 and 69 days. The case is therefore close to a period doubling. Figure 8b displays the projection on the xz-plane. One notices also here the two timescales.

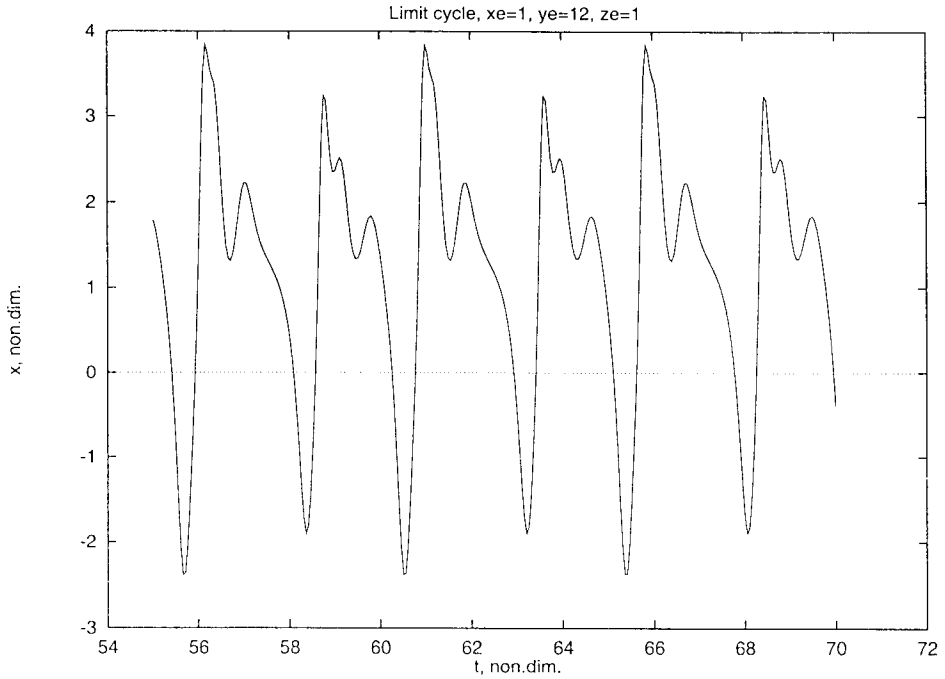

Fig. 8a. Another case with two time scales of 35 and 69 days for $x_E = 1$, $y_E = 12$, and $z_E = 1$. The amplitude of the x-component as a function of time.

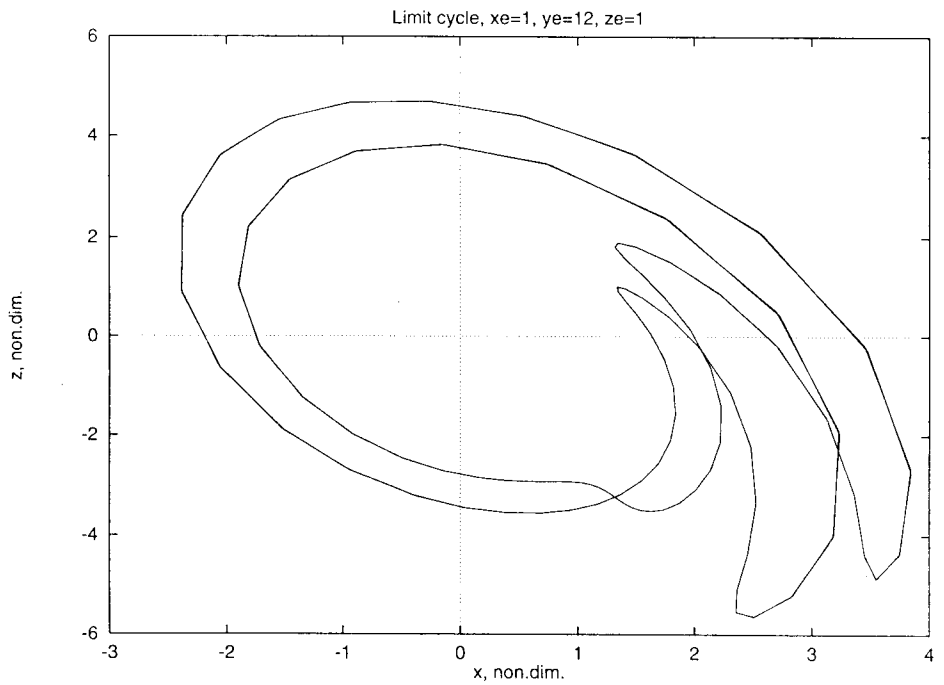

Fig. 8b. The projection of the limit cycle on the xz-plane. The two time scales are seen.

The examples displayed above indicate that the simple model is capable of producing limit cycles with periods corresponding to the major observed periods in intermonthly oscillations. On the other hand, it is also evident that other periods appear for a different selection of the forcing parameters. These periods are all longer than the dissipation time, although they do not agree exactly with the periods obtained from observational studies they have a strong tendency to cluster around the values of 30-35, 40-50 and 65-75 days except when small values are used for the forcing on the middle component. In the integrations we have found the 30 to 35 day oscillation as a sub-harmonic of a 70 day oscillation.

It appears therefore likely that the nonlinear interactions connected with the advection term are a main contributor to the creation of the observed inter-monthly oscillations. The condition for the creation of the limit cycle is first of all that the forcing shall be suitable selected within certain intervals which in this paper has been determined only for the simple case where the forcing is only on the middle component. However, the numerical experiments indicate clearly that if the forcing is selected close to the lower or upper limit of the interval we get a limit cycle with a small range while a larger range is obtained when the forcing is selected in the middle of the the interval. If oscillations should be detected in the atmosphere they need to be of a certain magnitude. It is apparently only the 30-35, 45 and 70 day oscillations that has been determined because of their larger amplitudes.

4. A barotropic model

As pointed out earlier Wiin Christensen and Wiin-Nielsen (1996) showed a single example of a stable limit cycle in a six component barotropic model with Newtonian forcing. The amplitudes are denoted x_1, y_1, x_2, y_2, x_3 and y_3 while the forcing components have an additional subscript of E. The period was 36 days.

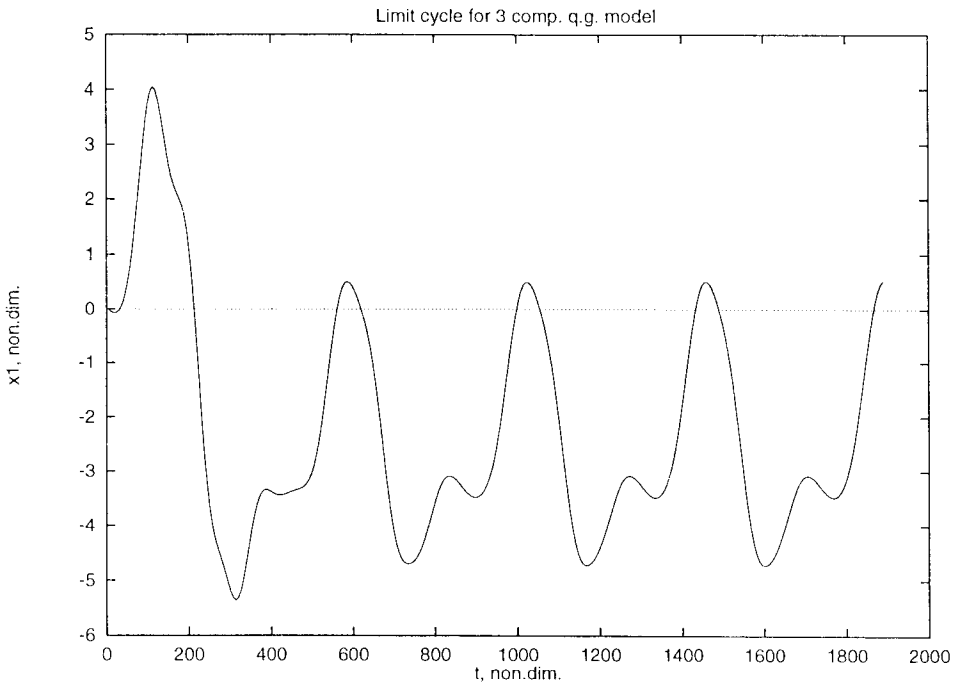

Fig 9. x_1 as a function of time in the barotropic model for $x_{1E} = -1.0x10^{-3}$, $x_{2E} = 1.9x10^{-2}$ and $x_{3E} = 3.0x10^{-2}$. The period is about 68 days.

The model is formulated on the spherical Earth, and it contains wave-wave interactions only. In the following we shall demonstrate that the model contains larger scales as well. The first example was integrated with $x_{1E} = -1.0x10^{-3}$, $x_{2E} = 1.9x10^{-2}$ and $x_{3E} = 2.9x10^{-2}$, while the forcing was zero on all three y-components. Note, that the scaling is different in this case because the dependent variables are streamfunction amplitudes. The variable x_3 is shown as a function of the non-dimensional time in Figure 9. The main period corresponds to about 68 days, but it is seen that an oscillation with a smaller period may be present. To bring out the oscillations with the smaller periods other experiments were conducted. Figure 10 was obtained from $x_{1E} = -1.0x10^{-3}$, $x_{2E} = 3.4x10^{-2}$ and $x_{3E} = 3.0x10^{-2}$. The main period is about 59 days, and the oscillation with a smaller time scale has become more pronounced. The two oscillations appear with about the same amplitude in Figure 11 obtained with the following forcing: $x_{1E} = 1.0x10^{-3}$, $x_{2E} = 2.2x10^{-2}$ and $x_{3E} = 4.2x10^{-2}$. The larger period is still 59 days, but the smaller period corresponds to about 32 days. Note that in these integrations the time scaling is different from the model in the previous sections. We use now:

$$t = \Omega^{-1}\tau \tag{4.1}$$

It is thus seen that both long and short periods are possible using the present barotropic model, and that these periods are of the correct order of magnitude.

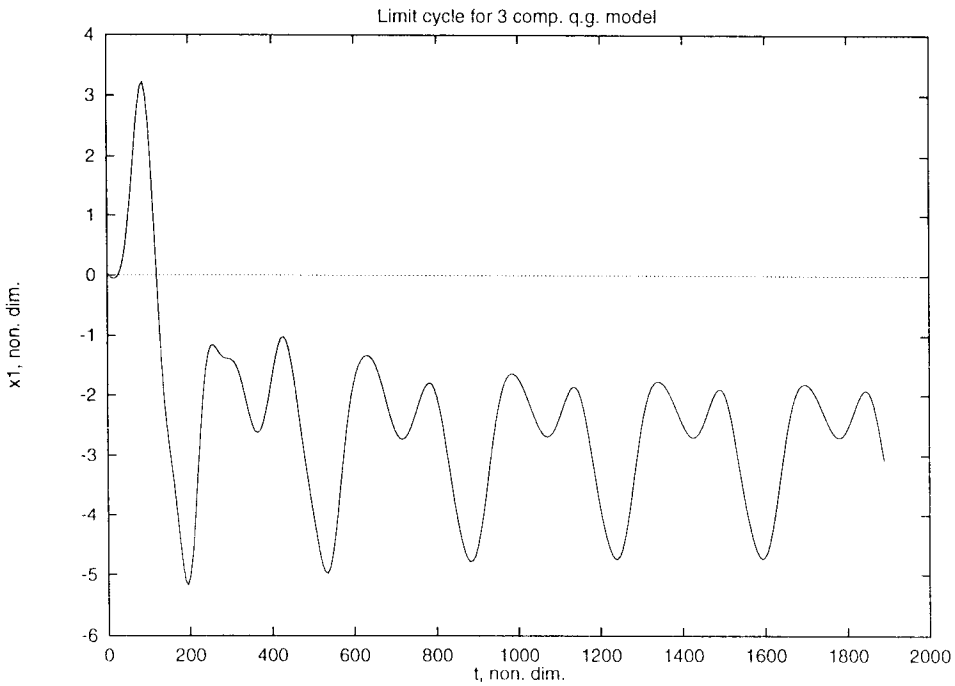

Fig. 10. x_1 as a function of time in the barotropic model for $x_{1E} = -1.0x10^{-3}$, $x_{2E} = 3.4x10^{-2}$ and $x_{3E} = 3.0x10^{-2}$. The periods is about 59 days.

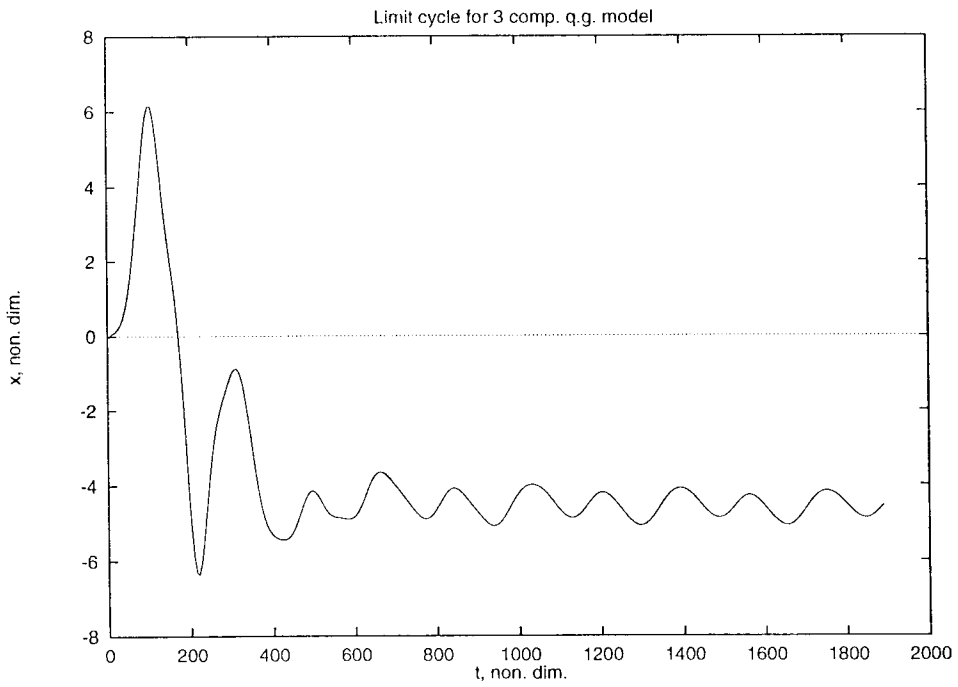

Fig. 11. x_1 as a function of time in the barotropic model for $x_{1E} = -1.0x10^{-3}$, $x_{2E} = 2.2x10^{-2}$ and $x_{3E} = 4.2x10^{-2}$. Periods are 59 and 32 days.

5. Concluding remarks

The present investigation has used a very simple model to investigate the longer term response to a Newtonian forcing. The study has been restricted to a low order model with one space dimension and time. The displayed examples are all of the limit cycle type, and it has been found that the periods of the limit cycles are close to the periods of the observed oscillations for selected values of the forcing parameters indicating that the nonlinear interactions may be responsible for the observed oscillations provided the forcing is of the required magnitude. More definite conclusions are probably not possible from the present study.

In view of the results obtained in the investigation one may wonder why no oscillation with a time scale of about 22.5 days have been recorded in data studies. The reason is probably that the response is too small to be observed using atmospheric data.

In the study we have assumed that the forcing parameters are constants with respect to time. In reality one would expect variations with time, but we do not know how to specify the time variations in a realistic way. It has, however, been investigated if an annual variation of the forcing has an impact on the oscillations. With a relatively small annual variation it is found that the impact on the various oscillations is very small supposedly due to the large annual period as compared to the periods of the various limit cycles. Due to the simplicity of the model it would be of interest to investigate the response of a higher order general circulation model to an observed spatial distribution of the heating.

REFERENCES

Barnett, T. P. and R. W. Preisemdorfer, 1978. Multifield analog prediction of short-term climate fluctuations using a climate state vector, *J. Atmos. Sci.*, **35**, 1771-1787.

Charney, J. G. and J. G. DeVore, 1979. Mutiple flow equilibria in the atmosphere and blocking, *J. Atmos. Sci.*, **36**, 1205-1216.

Itoh, H., 1985. The formation of quasi-stationary waves from the viewpoint of bifurcation theory, *J. Atmos. Sci.*, **42**, 917-932.

Källén, E. and A. Wiin-Nielsen, 1980. Non-linear, low-order interactions, *Tellus*, **32**, 393-409.

Legras, B. and M. Ghil, 1985. Persistent anomalies, blocking, and variations in atmospheric predictability, *J. Atmos. Sci.*, **42**, 433-471.

Legras, B., T. Desponts, and B. Piguet, 1987. Cluster analysis and weather regimes, Proc. ECMWF Workshop on the nature and prediction of extra-tropical weather regimes. Vol.2, ECMWF, Reading, Shinfield Park, U.K.

Lorenz, E. N., 1963. Deterministic nonperiodic flow, *J. Atmos. Sci.*, **20**, 130-141.

Madden, R. A. and P. R. Julian, 1971. Detection of a 40-50 day oscillation in the zonal wind in the tropical Pacific, *J. Atmos. Sci.*, **28**, 702-708.

Mo, K. C. and M. Ghil, 1987. Statistics and dynamics of persistent anomalies, *J. Atmos. Sci.*, **44**, 877-901.

Mo, K. C. and M. Ghil, 1988. Cluster analysis of multiple planetary flow regimes, *J. Geophys. Res.*, **93**, 10927-10951.

Molteni, F., L. Ferranti, T. N. Palmer, and P. Viterbo, 1993. A dynamical interpretation of the global response to equatorial Pacific SST anomalies, *J. Climate*, **6**, 777-795.

Obukhov, A. M., 1974. Global invariants of atmospheric motion, Physical and Dynanmic Climatology, World Meteorological Organization, 106-112.

Plaut, G. and R. Vautard, 1994. Spells of low frequency oscillations and weather regimes in the Northern Hemisphere, *J. Atmos. Sci*, **51**, 210-236.

Preisendorfer, R. W., 1988. Principal Component Analysis in Meteorology and Oceanography, C.D. Mobley, Ed., Elsevier, 425 pp.

Reinhold, B. B. and R. T. Pierrehumbert, 1982. Dynamics of weather regimes: Quasi-stationary waves and blocking, *Mon. Wea. Rev.*, **110**, 1105-1145.

Vautard, R. and B. Legras, 1988. On the source of midlatitude low-frequency variability, Part II: Nonlinear equilibration of weather regimes, *J. Atmos. Sci.*, **45**, 2845-2867.

Wallace, J. M. and D. S. Gutzler, 1981. Teleconnection in the geopotential height field during the Northern Hemisphere winter, *Mon. Wea. Rev.*, **109**, 784-812.

Wiin Christensen, C. and A. Wiin-Nielsen, 1996. Blocking as a wave-wave interaction, *Tellus*, **48A**, No. 2, 254-271.

Wiin-Nielsen, A., 1975. Predictability and climate variation illustrated by a low-order system, ECMWF seminar on the scientific foundation of medium-range forecasts, Part I, 258-306.

Wiin-Nielsen, A., 1979. Steady states and stability properties of a low-order barotropic system with forcing and dissipation, *Tellus*, **31**, 375-386.